The following supplement accompanies the article

Spatial variability in responses to environmental conditions in Southern Hemisphere long-finned pilot whales

Vicki Hamilton*, Karen Evans, Ben Raymond, Emma Betty, Mark A. Hindell

*Corresponding author: vicki.hamilton@utas.edu.au

Marine Ecology Progress Series 629: 207–218 (2019)

Table S1. Growth layer group (GLG) estimates established using standard repeat count age estimation procedures ('Initial estimate') and revised age estimates following modified visual crossdating ('Revised estimate') for two teeth from each long-finned pilot whale(s) *Globicephala melas* (n = 30) stranded at Rakiura, New Zealand (ID R-) and King Island, Tasmania, Australia (ID KI-)

Tooth ID#	Initial estimate	Revised estimate	Adjustment
R-GM1-1	13	13	0
R-GM1-2	12	13	+1
R-GM2-3	13	13	0
R-GM2-4	14	13	−1
R-GM3-3	12	12	0
R-GM3-4	12	12	0
R-GM4-2	9	9	0
R-GM4-3	10	9	−1
R-GM5-1	8	8	0
R-GM5-2	8	8	0
R-GM6-1	10	10	0
R-GM6-2	10	10	0
R-GM7-1	11	11	0
R-GM7-3	10	11	+1
R-GM8-2	7	7	0
R-GM8-3	6	7	+1
R-GM9-2	7	7	0
R-GM9-3	7	7	0
R-GM10-1	12	12	0
R-GM10-4	10	12	+2
R-GM11-3	6	6	0
R-GM11-4	6	6	0
R-GM12-1	11	11	0
R-GM12-4	10	11	+1
KI-GM1-1	8	8	0
KI-GM1-2	8	8	0
KI-GM2-1	9	9	0

KI-GM2-2	8	9	+1
KI-GM3-1	13	13	0
KI-GM3-2	13	13	0
KI-GM4-1	12	12	0
KI-GM4-2	12	12	0
KI-GM5-1	10	10	0
KI-GM5-2	9	10	+1
KI-GM6-1	11	11	0
KI-GM6-2	11	11	0
KI-GM7-1	10	10	0
KI-GM7-2	7	10	+3
KI-GM9-1	17	16	−1
KI-GM9-2	16	16	0
KI-GM10-1	6	6	0
KI-GM10-2	6	6	0
KI-GM11-1	7	7	0
KI-GM11-2	6	7	+1
KI-GM12-1	14	14	0
KI-GM12-2	14	14	0
KI-GM13-1	12	14	+2
KI-GM13-2	14	14	0
KI-GM14-1	12	12	0
KI-GM14-2	12	12	0
KI-GM15-1	8	8	0
KI-GM15-2	9	8	−1
KI-GM16-1	8	8	0
KI-GM16-2	8	8	0
KI-GM21-1	8	8	0
KI-GM21-2	8	8	0
KI-GM28-1	8	8	0
KI-GM28-2	8	8	0
KI-GM29-1	13	13	0
KI-GM29-2	13	13	0

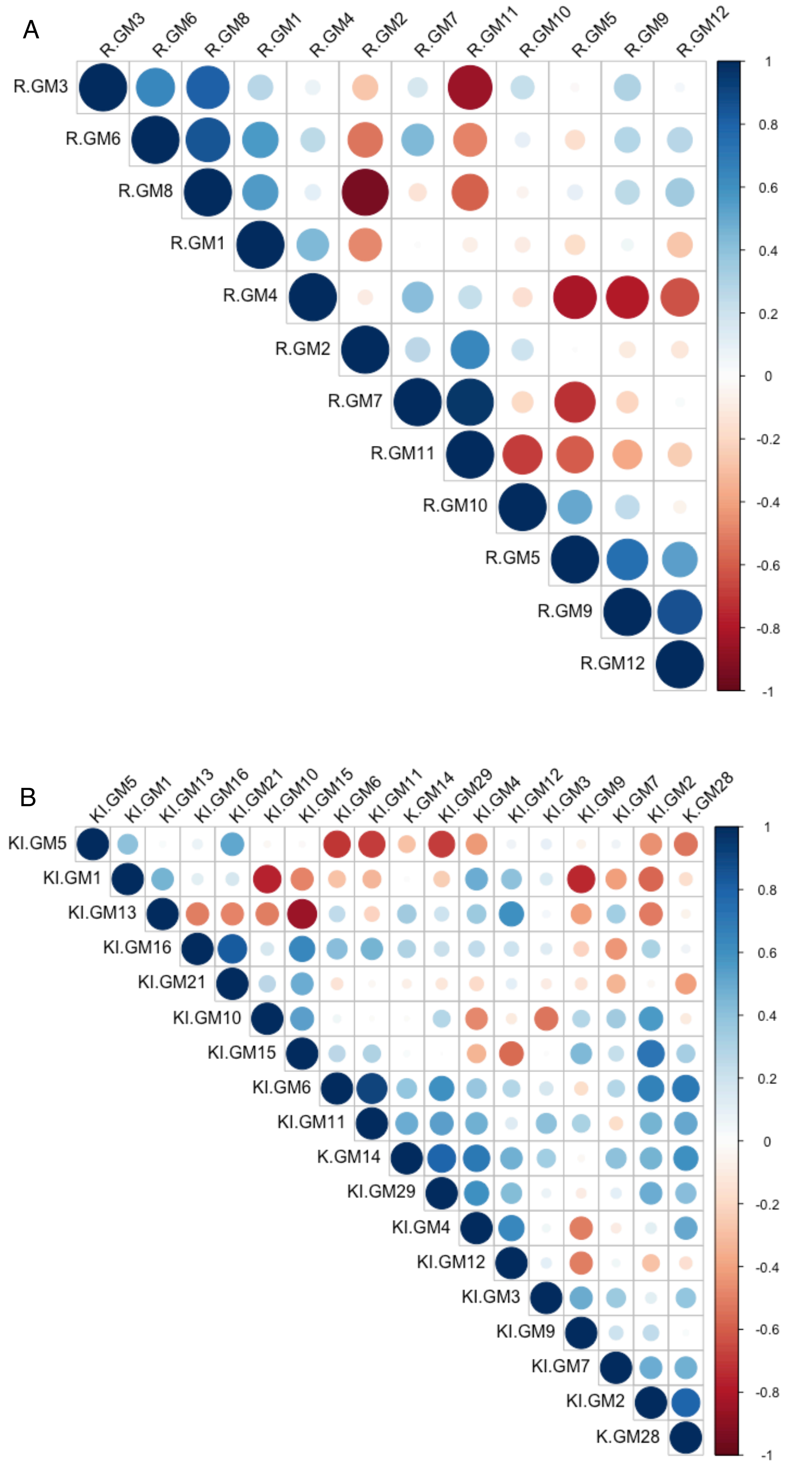

Fig. S1. Correlation matrix (Pearson's) comparing individual tooth growth chronologies of long-finned pilot whales *Globicephala melas* from (A) New Zealand and (B) Australia. The colour and size of circles are proportional to the correlation coefficient values

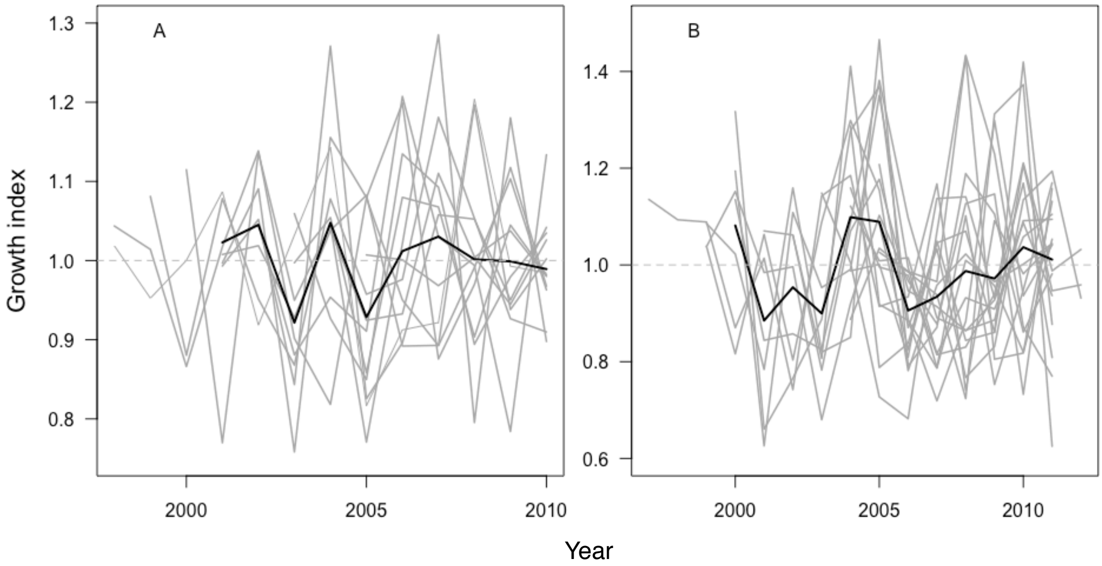

Fig. S2. Tooth growth chronologies of individuals (grey lines) and master chronologies (black line) for long-finned pilot whales *Globicephala melas* from (A) New Zealand (n = 12) and (B) Australia (n = 18). Dashed horizontal line: the mean

Table S2. Environmental data used in models and spatial correlations

Climate index/environmental variable	Time period	Source	Resolution
Southern Annular Mode Index (SAM)	2000–2011	https://climatedataguide.ucar.edu/climate-data/marshall-southern-annular-mode-sam-index-station-based (Marshall 2016)	Annual values
Southern Oscillation Index (SOI)	2000–2011	Australian Bureau of Meteorology (http://www.bom.gov.au/climate/current/soi2.shtml)	Annual means calculated from the monthly values
Indian Ocean Dipole (IOD)	2000–2011	https://www.esrl.noaa.gov/psd/gcos_wgsp/Timeseries/DMI/ (http://www.jamstec.go.jp/frcgc/research/d1/iod/e/iod/about_iod.html)	Annual means calculated from the monthly values
Sea surface temperature (SST, °C), NOAA ERSST v5	2000–2011	https://www.esrl.noaa.gov/psd/data/gridded/data.noaa.ersst.v5.html	Seasonal averages calculated from monthly values, 2° spatial resolution
Zonal wind speed, NCEP/NCAR Reanalysis	2000–2011	https://www.esrl.noaa.gov/psd/data/gridded/data.ncep.reanalysis.derived.surface.html	Seasonal averages calculated from monthly values, 2.5° spatial resolution

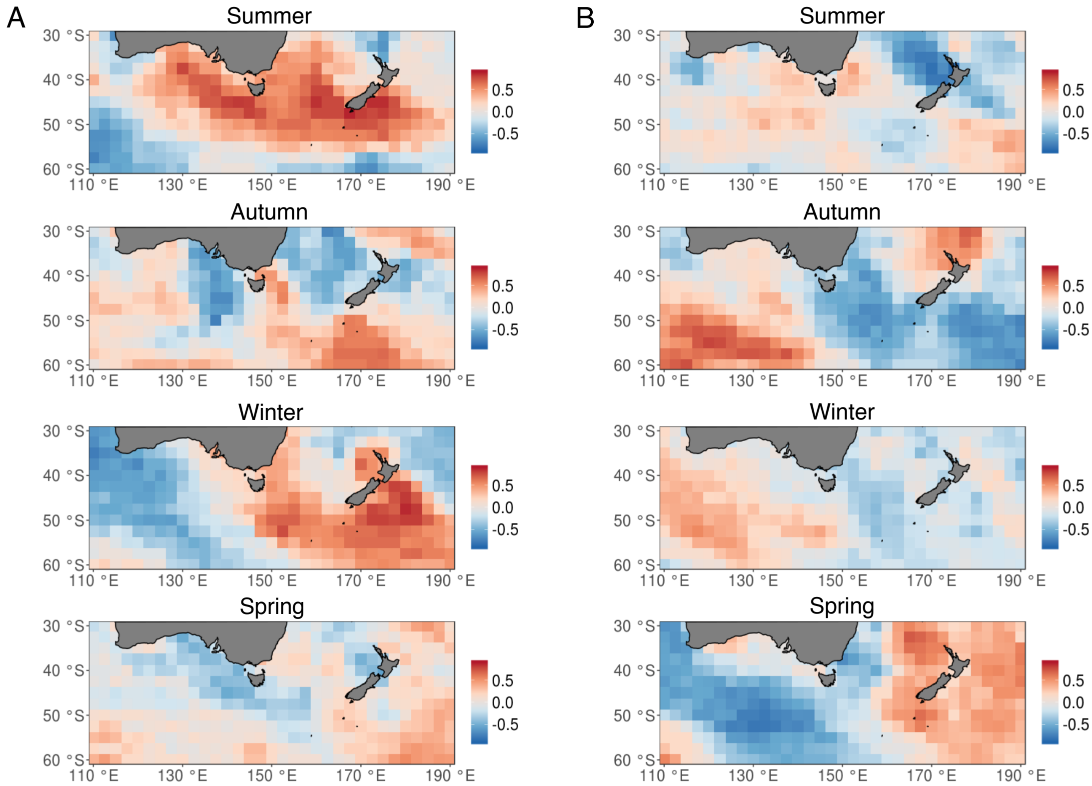

Fig. S3. Spatial maps of correlations between gridded seasonal averages (austral summer: Dec, Jan, Feb; autumn: Mar, Apr, May; winter: Jun, Jul, Aug; spring: Sep, Oct, Nov) of zonal wind speed and long-finned pilot whale (*Globicephala melas*) tooth growth chronologies from (A) New Zealand (2001–2010) and (B) Australia (2000–2011). Red shades: positive correlations; blue shades: negative correlations

Text S1. Additional crossdating, detrending and chronology details

Adjustment to GLG identification via modified visual crossdating within individuals
Cross-checks of distinctive growth layer groups (GLGs) among teeth from the same individuals resulted in GLG adjustments of −1 to +3 GLGs in a single tooth from each of 14 pilot whales (Table S1). The modal GLG adjustment was +1 GLG, associated with missing a GLG by misidentification of a GLG as an accessory layer. The modified visual crossdating process also assisted in the identification of GLG boundaries including that associated with the pulp cavity margin.

Statistical crossdating among individuals
GLG width time series were statistically crossdated following Hamilton & Evans (2018) to check similar patterns of GLG widths correlated among samples, as an additional step to aid correct calendar year assignment of GLGs. If potential errors in GLG width time series were identified during the crossdating process, the tooth image the time series was derived from was visually re-examined and corrections were made to the GLG width time series only if an error in GLG identification could be verified on the original image of the tooth.

Four New Zealand time series and seven Australian pilot whale time series were not sufficient in length (≤ 8 GLGS) to effectively correlate back to the pilot whale mean time series for each stranding group, and so crossdating was not carried out on these individuals. Six New Zealand pilot whale time series and eight time series for Australian pilot whales returned poor correlation values ($p \geq 0.05$) and were re-examined for potential errors. Interseries correlation values for each stranding were 0.529 for New Zealand and 0.464 for Australian pilot whales before crossdating.
Errors in GLG identification were located and corrected for one pilot whale GLG width time series from New Zealand (GLG at the pulp cavity margin had been misidentified as incomplete) and two pilot whale GLG width time series from Australia contained an error in GLG identification (falsely added GLGs).
After correction of errors, poor correlations ($p \geq 0.05$) remained for five New Zealand pilot whale time series and four Australian pilot whale time series. The interseries correlation values for each stranding improved overall, reflecting the corrections made, 0.621 for New Zealand and 0.523 for Australian pilot whales.

After crossdating checks and any adjustments to GLG identification, the raw GLG width time series were detrended to remove age-related trends in GLG width time series or variability specific to an individual, thereby enhancing detection of a common, population-wide signal (Fritts 1976, Cook et al. 1990).

Detrending
Linear models, negative exponential curves and different flexibilities of cubic smoothing splines were applied to both the New Zealand and Australian pilot whale time series to determine the best detrending method to standardise GLG width time series and enhance a common signal for each stranding group.

A decreasing trend in GLG widths was observed in the Australian pilot whale time series, resulting in a good fit of negative linear or negative exponential curves to the early portions of individual time series. Departures from the exponential model in the latter parts of time series were best fit by cubic smoothing splines. Subsequently a ‘double detrending’ method as described by Cook (1985) was used for pilot whales from Australia, in which GLG width time series were first detrended by negative exponential curves or negative linear regression models and then the indexed time series were detrended once more using cubic smoothing splines. Although a decreasing trend in GLG widths was also observed in the New Zealand pilot whale time series, negative exponential curves did not provide a good fit to all individual time series, resulting in ‘end effects’ for time series (i.e. poor fits at either end of the individual time series, leading to inflated indices when converted to standardised measurements). Although negative exponential detrending returned a higher $\bar{r}$ value for New Zealand pilot whale time series, visual inspection revealed that cubic smoothing splines with a frequency response of 50% at a wavelength of n-years/2 provided a better fit to the data (second highest $\bar{r}$ value).

Each individual’s raw GLG width measurement time series was standardised by dividing the measured GLG width for each year by the value predicted from the spline, thereby resulting in a chronology for each individual comprised of a unitless growth index with mean of 1 (Cook et al. 1990, Black et al. 2005).

$$\text{Growth Index (GI)} = R_t / G_t$$

where R_t and G_t are the actual (measured) and predicted widths at year *t*.

Chronologies

Although there was relatively high individual variability, individuals did show some synchrony, which was reflected in the master chronologies. This included above average (> 1.0) growth across most individuals from New Zealand in 2004, and across most individuals from the Australian stranding in 2004 and 2005 (Fig. S2). Most individuals from New Zealand had below average (< 1.0) growth in 2003 and 2005 and those from Australia had below average growth in 2003 and 2006 (Fig. S2).

LITERATURE CITED

Black BA, Boehlert GW, Yoklavich MM (2005) Using tree-ring crossdating techniques to validate annual growth increments in long-lived fishes. Can J Fish Aquat Sci 62:2277-2284

Cook E, Briffa K, Shiyatov S, Mazepa V, Jones P (1990) Data analysis. In: Cook ER, Kairiukstis LA (eds) Methods of dendrochronology: Applications in the environmental sciences. Kluwer Academic Publishers, Dordrecht, p 97–162

Cook ER (1985) A time series analysis approach to tree ring standardization. PhD Thesis. University of Arizona, Tucson, AZ

Fritts H (1976) Tree rings and climate. Academic, San Diego, California

Hamilton V, Evans K (2018) Establishing growth chronologies from marine mammal teeth: A method applicable across species. J Exp Mar Biol Ecol 505:24-34

Marshall GJ (2016) The Climate Data Guide: Marshall Southern Annular Mode (SAM) Index (Station-based). Available on: https://climatedataguide. ucar. edu/climate-data/marshallsouthern-annular-mode-sam-index-station-based [Accessed: 13 February 2018]